

UNCLASSIFIED

AD NUMBER

AD049092

LIMITATION CHANGES

TO:

Approved for public release; distribution is unlimited.

FROM:

Distribution authorized to U.S. Gov't. agencies and their contractors;
Administrative/Operational Use; MAR 1954. Other requests shall be referred to Wright Air Development Center, Wright-Patterson AFB, OH 45433.

AUTHORITY

AFAL ltr, 27 Dec 1979

THIS PAGE IS UNCLASSIFIED

THIS REPORT HAS BEEN DELIMITED
AND CLEARED FOR PUBLIC RELEASE
UNDER DOD DIRECTIVE 5200.20 AND
NO RESTRICTIONS ARE IMPOSED UPON
ITS USE AND DISCLOSURE.

DISTRIBUTION STATEMENT A

APPROVED FOR PUBLIC RELEASE,
DISTRIBUTION UNLIMITED.

Armed Services Technical Information Agency

AD

49092

NOTICE: WHEN GOVERNMENT OR OTHER DRAWINGS, SPECIFICATIONS OR OTHER DATA ARE USED FOR ANY PURPOSE OTHER THAN IN CONNECTION WITH A DEFINITELY RELATED GOVERNMENT PROCUREMENT OPERATION, THE U. S. GOVERNMENT THEREBY INCURS NO RESPONSIBILITY, NOR ANY OBLIGATION WHATSOEVER; AND THE FACT THAT THE GOVERNMENT MAY HAVE FORMULATED, FURNISHED, OR IN ANY WAY SUPPLIED THE SAID DRAWINGS, SPECIFICATIONS, OR OTHER DATA IS NOT TO BE REGARDED BY IMPLICATION OR OTHERWISE AS IN ANY MANNER LICENSING THE HOLDER OR ANY OTHER PERSON OR CORPORATION, OR CONVEYING ANY RIGHTS OR PERMISSION TO MANUFACTURE, USE OR SELL ANY PATENTED INVENTION THAT MAY IN ANY WAY BE RELATED THERETO.

Reproduced by
DOCUMENT SERVICE CENTER
KNOTT BUILDING DAYTON 2 OHIO

UNCLASSIFIED

AD No. 49 092

ASTIA FILE COPY

WRIGHT AIR DEVELOPMENT CENTER
TECHNICAL REPORT 54-173
PART 1

092

ALUMINA-BASE CERMETS

THOMAS S. SHEVLIN
CHARLES A. HAUCK

THE OHIO STATE UNIVERSITY RESEARCH FOUNDATION

MARCH 1954

WRIGHT AIR DEVELOPMENT CENTER

WADC TECHNICAL REPORT 54- 173
PART 1

ALUMINA-BASE CERMETS

*Thomas S. Shevlin
Charles A. Hauck*

The Ohio State University Research Foundation

March 1954

Aeronautical Research Laboratory
Contract No. AF 33(616) - 472
Task No. 70634

Wright Air Development Center
Air Research and Development Command
United States Air Force
Wright-Patterson Air Force Base, Ohio

FOREWORD

This report was prepared by Thomas S. Shevlin and Charles A. Hauck of the Ohio State University Research Foundation, Columbus, Ohio, under the general supervision of J.C. Everhart, Supervisor of Ceramic Research. This report summarizes work on this contract during the period 1 March 1953 to 1 March 1954 in which time studies were conducted on alumina-base cermets. This work is to be continued and further reports will be issued as warranted by the progress.

This work was accomplished under Contract AF 33(616)-109. It was administered under the direction of the Aeronautical Research Laboratory/ with Murray A. Schwartz as project engineer, and is identified under Task No. 70634, "Ceramic and Cermet Research".

ABSTRACT

Preparation, test procedure, and physical properties of a cermet composed of 34% Al_2O_3 - 66% (80Cr-20Mo), in addition to modified compositions, are described. Properties evaluated include firing shrinkage, density, modulus of rupture, tensile strength, stress-rupture, modulus of elasticity, oxidation resistance, thermal shock resistance, and hardness. X-ray studies were conducted to determine solid solution effects. The cermet studied had a 1000-hour stress-rupture life at 1800°F of 19,000 psi, negligible oxidation to 2000°F and excellent thermal shock resistance at 1900°F. This material is being evaluated for nozzle vane and flame holder applications.

PUBLICATION REVIEW

This report has been reviewed and is approved.

FOR THE COMMANDER:



Leslie B. Williams
Colonel, USAF
Chief, Aeronautical Research
Laboratory
Directorate of Research

TABLE OF CONTENTS

	<u>Page</u>
I INTRODUCTION.....	1
II MATERIALS.....	4
III COMPOSITIONS.....	5
IV PREPARATION OF BATCH.....	6
V FORMING.....	7
Specimen Types.....	7
Operations.....	8
VI FIRING.....	10
Furnaces.....	10
Atmosphere.....	10
Temperature.....	12
Soft Sintering.....	12
VII PROPERTY EVALUATIONS.....	12
Firing Shrinkage.....	12
Density.....	13
Modulus of Rupture.....	13
Tensile Strength.....	17
Stress Rupture.....	17
Modulus of Elasticity.....	18
Oxidation Resistance.....	18
Impact Resistance.....	19
Thermal Shock Resistance.....	19
Thermal Expansion.....	21
Metallography.....	25
Hardness.....	26
X-ray Studies.....	26
VIII DISCUSSION.....	28

LIST OF TABLES

Table No.	Page
I Physical Properties of A-355.6-G.....	3
II Batch Compositions.....	5
III Density of "AC" Series Specimens.....	13
IV Modulus of Rupture of A-355.6-G at Various Temperatures.....	14
V Modulus of Rupture of AT355.6-G and AZ-355.6-G.....	15
VI Modulus of Rupture of AC Series Specimens at 75°F.....	16
VII Modulus of Rupture of AC Series Specimens at 2000°F.....	16
VIII Tensile Strength of A-355.6-G from 75°F to 2400°F.....	17
IX Stress Rupture Data for A-355.6-G at 1800°F and 2000°F.....	18
X Oxidation of A-355.6-G at 2000°F.....	19
XI Thermal Shock Endurance of A-355.6-G Nozzle Diaphragm Blades.....	20
XII Thermal Expansion of A-355.6-G.....	21
XIII Thermal Expansion of Cr.....	22
XIV Thermal Expansion of 80Cr-20Mo.....	23
XV Thermal Expansion of Al ₂ O ₃ and Al ₂ O ₃ plus Cr ₂ O ₃	25

LIST OF ILLUSTRATIONS

Figure	<u>Page</u>
1 Flame Holder and Forming Accessories	35
2 Oxidation and Reduction of Chromium Oxides Related to Dew Point and Firing Temperature.....	36
3 Porosity and Modulus of Rupture versus Firing Temperature for Composition A-355.6-G.....	37
4 Modulus of Rupture versus Test Temperature for A-355.6-G.....	38
5 Tensile Strength versus Test Temperature for A-355.6-G.....	39
6 Stress Rupture in Tension for A-355.6-G.....	40
7 Oxidation of A-355.6-G at 2000°F.....	41
8 Thermal Expansion Data for 80Cr-20Mo, Cr, A-355.6-G, and Al_2O_3 (Al_2O_3 and $Al_2O_3+Cr_2O_3$)	42
9 Thermal Expansion Furnace and Reference System.....	43
10 Normal Structure of A-355.6-G at 200X.....	44
11 Globuliferous Structure of A-355.6-G Containing Milling Impurities, 200X.....	44
12 Segregation in A-355.6-G Rod Specimen No. 9, 25X.....	45
13 Structure of A-355.6-G Nozzle Diaphragm Blade No. 4. Poorest Microstructure Observed. 25X.....	45

INTRODUCTION

The development, properties, and related investigations pertaining to a cermet containing 34.4% alumina and 65.6% 80Cr-20Mo alloy were undertaken because previously developed Al_2O_3 - Cr cermets¹ containing approximately equal volumes of Al_2O_3 and Cr displayed a certain marginal thermal shock deficiency. Thermal shock resistance was considered capable of improvement by replacing the Cr with an alloy of Cr and Mo. The 80Cr-20Mo alloy was selected because Cr and Mo form a solid solution alloy², because of certain theoretically predictable features ascribed to such an alloy, and because both early laboratory experiments and published literature³ indicated potentially satisfactory oxidation resistance properties.

Using Cr as the basis of comparison it is logical theoretically to predict a lower thermal expansion in a Cr-Mo solid solution. This means that the alloy could be expected to produce a better thermal expansion match between the Al_2O_3 and the metal phase than that which exists in Cr- Al_2O_3 cermet bodies, because the thermal expansion of Cr is slightly higher than that of Al_2O_3 and the addition of relatively low expanding Mo to Cr forming a solid solution should lower the thermal expansion of the metal phase. The alloy 80Cr-20Mo was selected because it was thought that this alloy might be reasonably close to Al_2O_3 in thermal expansion. The minimizing of thermal stresses by effecting a thermal expansion match between phases was considered capable of raising the thermal shock resistance.

Again using Cr as the basis for comparison, addition of Mo in a solid solution alloy should amount to increasing the strength of the metal phase in the temperature range 1800°F to 2200°F, because alloys are generally stronger than pure metals where there are no eutectics, and because a high hot-strength contribution would be expected from high-melting Mo notwithstanding the fact that Mo additions to Cr produce a depression of the liquidus at temperatures approximately 1000°F above the anticipated use temperature of the alloy as the cermet metal phase. An improved high temperature strength was thus predicted, and a consequent improvement in thermal shock resistance was forecast.

Thermal conductivity should be higher for Cr-Mo alloys than for Cr, because Mo has a higher thermal conductivity than Cr and in substitutional solid solution alloys the rule of mixtures applies quite well. Thermal shock resistance should be improved as a result of this fact.

It was postulated that a wetting reaction between Al_2O_3 and a Cr-Mo alloy could operate in much the same way as between Al_2O_3 and Cr, through preferential oxidation of the Cr in the alloy. The basic hypothesis which has been advanced is that Cr can be bonded to Al_2O_3 if a limited amount of Cr_2O_3 is formed on the surface of the Cr (particle) followed by the solid solution of this Cr_2O_3 in Al_2O_3 .^{4,5} It has been shown that such a mechanism involving the preferential oxidation of Cr in stainless steel followed by the solution of the Cr_2O_3 product in Al_2O_3 can operate.⁶

An oxidation test at 1800°F of a single 95Cr-5Mo alloy was made in 1949 to obtain a preliminary insight into the oxidation resistance of Cr-Mo alloys. It showed that at least moderate contents of Mo in Cr-Mo solid solutions could be tolerated with respect to oxidation properties. Later review of the work of Parke and Bens⁷ covering alloys containing 60% Cr, 25% Mo, and 15% Fe revealed that such alloys could be stress-rupture tested in air at 1800°F without notable appearance of troublesome oxidation. It was tentatively inferred that an 80Cr-20Mo alloy containing approximately 50 volume percent of Al_2O_3 as a diluent should satisfactorily resist oxidation, and this was later seen to be the case.

Certain exploratory investigations were conducted in an attempt to discover how modification of the Al_2O_3 phase would affect the cermet properties. For this purpose calcined aluminum hydrate was used to obtain an extremely fine Al_2O_3 for incorporation in the body. Minor additions of ZrO_2 and TiO_2 were made in an attempt to alter favorably the wetting between metal and oxide phases.

The properties of the body composed of 34.4% Al_2O_3 plus 65.6% 80Cr-20Mo and designated A-355.6-G are given in Table I. As a result of the development and testing leading to these data, it can be said that high temperature strength, sustained load-carrying ability, and oxidation resistance are sufficiently high to justify consideration for gas turbine use. Adequacy of impact resistance is questionable in present design configurations. The effects of the composition modifications mentioned above are not conclusive at the present time.

Recent data obtained by the Refractories Section, National Bureau of Standards on a Cr- Al_2O_3 body previously described¹ and prepared in our laboratories indicates usability of the composition for flame holders.

Table I
Physical Properties of A-355.6-G

Firing shrinkage: 14%

Density: 5.83-5.90

Porosity: None detectable microscopically or by water boiling

Breaking strength:	Temp., °F	Mod. of Rup., psi	Tensile, psi
	75	87,640	53,000
	1600		40,350
	1800	58,000	28,500
	2000	45,500	25,000
	2200	45,500	18,600 min.
	2400	38,750	9,415

Stress rupture 1000 hour life:	Temp., °F	Tensile Stress, psi
	1800	19,000
	2000	4,000

Modulus of elasticity: 45×10^{-6}

Oxidation resistance: Excellent: 0.001 to 0.002 inch penetration in 1000 hrs at 2000°F. No low temperature oxidation.

Thermal shock resistance: Excellent. Withstands 1000 cycles of simulated burner blow-out from 1900°F in standard WADC test.

Thermal expansion:	Temperature range, °F	Coefficient 1/°F
	75- 500	3.05
	75-1000	4.68
	75-1500	4.56
	75-2000	5.33
	75-2400	5.93

II MATERIALS

The following materials were used in the preparation of compositions covered in this report.

Alumina: Corundum form, 0.05% maximum soda, Alcoa Grade T-61, milled to minus 25 microns acid leached and furnished by the Champion Spark Plug Company.

Chromium: Electrolytic, 99% minimum chromium content, minus 325 mesh, furnished by Charles Hardy, Inc. or Electro-metallurgical Division, Union Carbide and Carbon Corporation.

Molybdenum: Hydrogen reduced, 99.75 minimum molybdenum content, minus 200 mesh, furnished by Charles Hardy, Inc.

Aluminum Hydrate: Alcoa grade C-730, 24.7% combined water, minus 0.8 micron, 99% + pure, furnished by Aluminum Company of America.

TiO₂: Heavy grade, 200 mesh, furnished by Titanium Alloy Manufacturing Division of the National Lead Company.

ZrO₂: Electrically fused, 200 mesh unstabilized, furnished by Titanium Alloys Manufacturing Division of the National Lead Company.

Where a binder-lubricant was required in forming operations Carbowax "4000," furnished by the Carbide and Carbon Chemicals Company, Division of Union Carbide and Carbon Corporation was used.

III COMPOSITIONS

The compositions involved in the work under this contract are given in Table II below. The composition A-355.6-G received the most attention, and this report is primarily concerned with this composition.

Table II
Batch Compositions

Designation	Component	Weight %	Volume %
A-355.6-G	T-61 Alumina	34.4	50
	80Cr-20Mo*	65.6	50
AT-355.5-G	T-61 Alumina	34.0	50
	TiO ₂	1.0	
	80Cr-20Mo*	65.0	50
AZ-355.6-G	T-61 Alumina	34.0	50
	ZrO ₂	1.0	
	80Cr-20Mo*	65.0	50
AC-355.6-G	Calcined Aluminum hydrate	34.4	50
	80Cr-20Mo	65.6	50
A-373-G	Calcined aluminum hydrate	17	28
	80Cr-20Mo	83	72
AC-381-G	Calcined aluminum hydrate	9	16
	80Cr-20Mo	91	84
AC-385-G	Calcined aluminum hydrate	5	9
	80Cr-20Mo	95	91
390-G	80Cr-20Mo	100	100
A-16.14-G	T-61 Alumina	28.6	41.9
	Cr	71.4	58.1

*A diffusion alloy of 80% Cr and 20% Mo by weight.

IV PREPARATION OF BATCH

Batch preparation consists of an alloy or aluminum-hydrate preparation step and a milling and granulating step for the compositions which contain the alloy or the calcined hydrate. A-16.14-G, of course, does not require any preparation of ingredients, since the metal phase is Cr powder used as received, and the alumina is T-61 grade used as received.

In preparing the 80Cr-20Mo alloy, 80% by weight of Cr powder is mixed with 20% by weight of Mo powder in a glass container and agitated by hand for approximately 15 minutes. This mixture is placed in an alumina boat and fired to 3150° in a hydrogen atmosphere to be described below under FIRING. This temperature is somewhat higher than the temperature necessary for complete alloying by diffusion as indicated by x-ray analysis, but was employed because 3150° was indicated as the maturing temperature to be used for A-355.6-G in later studies, and it was considered desirable to form the alloy at a temperature as high as or higher than that of anticipated future heat treatment. The alloyed powder cake was broken into 4-mesh chunks in a steel mortar. These chunks were passed through a TYPE SH Mikro-Pluverizer which reduces coarse crystalline alloy to a fine powder, practically all of which will pass 200 mesh. The powder is incorporated into batches in this condition.

Calcined aluminum hydrate is prepared for those batches in which it is utilized, by firing to 2500°F and holding for 1 hour. A brief study was conducted to select a calcination temperature that would yield alpha Al_2O_3 in fine crystalline form. It was learned that heating for one hour at 2200°F produced kappa Al_2O_3 plus a small amount of alpha Al_2O_3 . Since there were no theta Al_2O_3 lines in the x-ray pattern of the 2200°F product, and Theta Al_2O_3 is a transition phase between kappa Al_2O_3 and alpha Al_2O_3 it was concluded that the kappa-theta transition is slow and the theta-alpha transition is fast at this temperature. Although it appeared that a longer time could yield 100% alumina, a higher temperature for calcination seemed preferable. Calcination at 2500°F for one hour produced only alpha Al_2O_3 as shown by the

x-ray pattern and microscopic examination showed crystals of the calcine to be all finer than 5 microns and most finer than 2 microns. Therefore, Alcoa C-730 calcined one hour at 2500°F as measured by thermocouples and pyrometric cones (cone 14 down) was used in those compositions of the "AC" series.

All compositions were mixed and ground together by placing weighed amounts of the batch ingredients totalling approximately 500 gm in one-quart capacity steel bass mills with approximately 12 pounds of tungsten carbide slugs of assorted sizes (less than 1 inch maximum dimension) as the grinding medium and 150cc of methyl alcohol as the liquid vehicle. After milling, the batches were air dried and granulated through a 65-mesh screen to produce a powder suitable for direct hydrostatic pressing. For forming bars involving steel die pressing it was necessary to use a temporary binder-lubricant to provide handling strength in the pressed condition. Carbowax "4000" was melted in a mortar and hot mixed into the body for this purpose, using an amount equal to 9% of the weight of dry batch. After hot mixing the wax into the body the batch was granulated through a 65-mesh screen preparatory to pressing.

V FORMING

a. Specimen Types

Four specimen types were used in the investigations covered by this report.

- (1) Bars 4.5 inches long by 0.5 inch wide by 0.15 inch thick.
- (2) Turbine nozzle diaphragm blades having an air-foil cross section with a 2.5 inch chord and a length perpendicular to the plane of the air-foil section equaling 3.9 inches.

- (3) Tensile test rods 9.5 inches long by 0.375 inch diameter gradually necked to a minimum diameter of 0.250 inch in the central 1.5 inches of the length.
- (4) Flame holders of hollow design and roughly triangular cross-section having a 3-inch length, a 1.15-inch height and a 1-inch base. The wall thickness, or distance from exterior surface to interior cavity, is approximately 0.1 inch. See Figure 1.

b. Forming Operations

Bar Specimens: Bar specimens were formed by pressing 65 mesh waxed batch material in a strip-case steel die having an opening 4.5 inches long by 0.5 inch wide. The die was charged and struck off, the thickness being controlled by the volume of the charge. After an initial low pressure application of approximately 1000 psi, die supports were removed, allowing the case to float and both punches to close on the charge from above and below. Pressures of approximately 10,000 psi were then employed, determined as the highest usable pressure which would provide handling strength without pressure cracking.

After this initial forming, the bars, placed in rubber envelopes and evacuated to approximately 1 mm of mercury, were repressed hydrostatically to 35,000 psi. This method produces a densely compacted green specimen free of pressure cracks.

Nozzle Diaphragm Blades: Both solid and hollow nozzle diaphragm blades were formed by hydrostatically pressing milled batch materials without using temporary binders or lubricants. In forming the solid blades, powder was charged into a thin-walled oversize rubber bag having the general shape of an airfoil, which was retained in a light-gage oversize metal can of roughly the same shape as an oversize finished blade. This assembly full of powder was vibrated, and as the powder compacted more was added.

After the assembly was full the rubber bag was closed with a rubber stopper and partially evacuated through a hypodermic needle inserted through the stopper. Evacuation brings about a slight compression of the powder and a certain rigidity of the powder and its rubber container as a unit. This permits the removal of the charged bag from the metal container. The evacuated assembly is then hydrostatically pressed at 35,000 psi to produce a binder free blank which can be shaped accurately with a sanding drum¹.

Initial attempts to form hollow nozzle diaphragm blades involved the use of a core. This was found to be unsatisfactory either because soft deformable materials such as paraffin or Wood's metal were too compressible and burst the surrounding compacted powder upon the release of hydrostatic pressure, or because hard steel, highly incompressible cores were bent when surrounded by an asymmetrical powder charge with non-ideal pressure distribution through the powder mass. A workable method was developed which consists of allowing the pressing fluid access to the core volume. This was accomplished by locating properly in the powder mass a Wood's metal core covered with a rubber envelope. After vibrating the powder into place, the lip of the outer rubber bag was sealed to the lip of the inner rubber envelope enclosing the Wood's metal, by rolling the two together. In order to provide a massive piece of rubber through which to evacuate this assembly by means of a hypodermic needle, the outer bag was stretched over a small rubber stopper located inside the bag near the top and sealed in place by wrapping the protruding surface with a rubber band from the outside. After evacuation the Wood's metal was melted and drained by placing the assembly in hot water. Hydrostatic pressing and finishing followed as with the solid blades.

Tensile Specimens: Rod specimens were formed by direct hydrostatic pressing of granulated batch material. A thin-walled rubber tube held within an outer perforated brass tube was filled with powder while the assembly was vibrated. One end of the tube was closed with a cylindrical movable rubber stopper before filling, the other was

closed with a shouldered rubber stopper after filling. The charge was evacuated with a hypodermic needle inserted through the shouldered stopper after filling; then the hole made by the needle was covered with grease and the assembly was subjected to a pressure of 35,000 psi. In this way rod specimens could be formed with good green strength and no temporary binder.

Rods consisting of A-355.6-G in the center section, and 70Al₂O₃-30Cr in the end sections were made in much the same way. This was done in the early stages of the investigation to conserve 80Cr-20Mo alloy used in A-355.6-G bodies. In charging, the tube was filled with the different compositions. Between the ends and the center section two mixtures of intermediate metal and Al₂O₃ content were used to form a graded join extending for a length of approximately 0.5 inch. A similar procedure has been described in detail for A-16.14-G1.

Flame Holders: A suitable method for forming hollow flame holders was found to consist of charging milled and granulated batch material around a centrally located and rather massive hardened steel core contained within a plastisol casing. Material is charged under vibration. After filling, the entire assembly is placed in a rubber bag, evacuated, and hydrostatically pressed at 35,000 psi. The core is easily withdrawn after pressing. The plastisol casing, steel core, green flame holder, and fired flame holder are shown in Figure 1.

After pressing, the ends of the flame holder are squared before templates are placed over the ends and positioned by means of shoulders which just fit into the opening formed by the core. The surface is formed to the contour of the templates by removing stock on a sanding belt. The templates are oversize to allow for a shrinkage of approximately 18% which was observed experimentally on early specimens formed in this way. This is slightly greater than the firing shrinkage observed after other hydrostatic press-forming operations which do not employ a core or a relatively thick outer casing. It is thought that these two features are responsible for a lower pressed density and a resulting high firing shrinkage.

VI FIRING

a. Furnaces

All specimen types were fired in furnaces consisting of a molybdenum-wound alumina tube appropriately insulated and contained within a gastight steel case. Bar specimens were fired in the 2-inch ID furnace⁸. Blades and flame holders were fired in the 6-inch ID furnace⁹. Rod specimens have been prefired in either furnace, as described below, but were fired to maturity in the 2-inch ID furnace only. During the course of investigations under this contract it was necessary to rebuild both furnaces, and in so doing the tightness of their cases was improved and provision was made for measuring the purity of the entering and exhaust gases used as the atmosphere during firing.

b. Atmosphere

The atmosphere employed in the firing of all specimens

was hydrogen purified by passing over copper turnings at 1000°F, through a tower of activated alumina, and over calcium chips at 600°F. Titanium hydride was used as a getter within the firing chambers of the furnaces to improve further the quality of the atmosphere.

The dew point of H_2 entering the furnaces has been observed to be consistently lower than 90°F. The dew point of exhaust gas has been measured and used as the dew point within the firing space, in an attempt to discern the probable oxidation reduction reactions involving Cr and its oxides. Dew points of the H_2 atmosphere within the furnaces, sampled at the furnace outlets throughout various firing cycles of both furnaces, are shown in Figure 2. Also shown are certain oxidation-reduction curves for chromium oxides, based on data of C. G. Maier¹⁰.

Consider first the curves based upon measured dew points: The upper curve (1) of this type is for the large molybdenum-wound resistor furnace. This curve shows the H_2O/H_2 ratio increase during the soaking period, caused by reduction of Cr_2O_3 , CrO or furnace refractories. The curve (2) nearly superimposed on this curve is for the small molybdenum-wound furnace based on determinations made soon after it was rebuilt. The intermediate curve (3) applies to the large molybdenum furnace, and merely indicates the spread on different runs. The lower curve (4) is based on later data obtained in connection with the small molybdenum-wound resistor furnace, and its relative position shows the atmosphere improvement with repeated firing. Dew points for the furnace atmospheres are shown extrapolated back to 1500°F. The extrapolation is supported in a general way by dew points measured in this temperature range, but with the exact temperature unknown. Optical pyrometer temperature measurements were not made in this low temperature range, but temperatures were estimated visually.

For the reduction reactions $Cr_2O_3 + 3H_2 \rightleftharpoons 2Cr + 3H_2O$, $Cr_2O_3 + H_2 \rightleftharpoons 2CrO + H_2O$, and $CrO + H_2 \rightleftharpoons Cr + H_2O$, the K_p or H_2O/H_2 ratios as a function of temperature from Maier's data were converted to dew points and plotted with the atmosphere dew point curves in Figure 2.

Considering Cr alone as the metal phase, the interpretation placed upon the information shown in Figure 2 is that in the low temperature portion of the firing cycle Cr is oxidizing to CrO and Cr_2O_3 . The relative amounts of the two oxides formed is unpredictable, being entirely dependent upon the relative rates of formation and entirely independent of equilibria considerations upon which the curves in Figure 2 are based. These curves indicate that the CrO which is formed cannot be oxidized further to Cr_2O_3 at any time during the firing cycle. Therefore, it must be reduced once again to Cr at the higher firing temperatures. The Cr_2O_3 which is

formed at low temperatures also can be reduced back to Cr at the higher temperature. It is known that this oxide, Cr_2O_3 , forms a complete series of solid solutions with Al_2O_3 , and that this solid solution takes place during firing of chromium alumina cermets.

While somewhat speculative at the present time, it is believed that similar reactions take place with Cr-Mo alloys, but that they involve Cr preferentially. It is known definitely that Cr_2O_3 - Al_2O_3 solid solutions are formed, and it is also known that hydrogen atmospheres of the purity determined are reducing with respect to all molybdenum oxides. Thus, in summary, it appears that Cr is oxidized to CrO and Cr_2O_3 at low temperatures, that Cr_2O_3 is both reduced and dissolved at higher temperatures, and that CrO is only reduced at higher temperatures not being further oxidized to Cr_2O_3 and thereafter dissolved in alumina. This leaves the possible roles of CrO in wetting and bonding unexplained, but does not preclude the operation of previously postulated concepts of the role of Cr_2O_3 in promoting bonding between Cr and Al_2O_3 .

c. Temperature

The optimum firing temperature for A-355.6-G was found to be 3150°F as indicated by porosity and modulus of rupture measurements at 750°F shown as a function of firing temperature in Figure 3. As previously reported¹, the optimum firing temperature for A-16.14-G has been determined as 3050°F to 3100°F . Less conclusive study indicates that the probable optimum maturing temperature for "AC" series specimens is 3000°F to 3050°F . For AT-355.6-G and AZ-355.6-G the maturing temperature of 3050°F was used, but was not determined to be the most suitable.

d. Preliminary Soft Sintering

Preliminary soft sintering followed by machine grinding was used as a technique to reduce the amount of difficult stock removal in the rod grinding operation following firing to maturity. A temperature of 2200°F was employed in this sintering operation.

VII PROPERTY EVALUATIONS

a. Firing Shrinkage

Linear firing shrinkage is determined as the ratio of the change in length on firing, to the unfired length. A value of 14% has been obtained for bar specimens of A-355.6-G.

A-16.14-G displays a firing shrinkage of approximately 15% as previously reported¹. Shrinkages of 15 to 16% were observed in AT-355.6-G and AZ-355.6-G. The firing shrinkages for the "AC" series specimens is 15 to 16%, and the overlap in values indicates that the differences in shrinkage for different compositions is not significant.

b. Density

The density calculated for A-355.6-G on the basis of the theoretical density of the solid solution alloy (7.65gm/cc based on x-ray measurements) and that of alumina (4gm/cc based on x-ray data) is 5.83 gm/cc. The density measured on two early specimens was 5.82 gm/cc, and in spot checks many later specimens show approximately this value of density.

The density of A-16.14-G is 5.85 gm/cc as previously reported¹.

The density of AT-355.6-G and AZ-355.6-G is assumed to be the same as that of A-355.6-G, namely 5.83gm/cc.

The calculated densities of "AC" series specimens based upon proportions of metal and alloy are given in Table III below.

Table III

Density of "AC" Series Specimens

Designation	Density, gm/cc
AC-355.6-G	5.83
AC-373-G	6.62
AC-381-G	7.07
AC-385-G	7.32

c. Modulus of Rupture

Modulus of rupture values as a function of test temperature were determined using bar specimens and a span to depth ratio of approximately 15 to 1. These are given in Table IV below.

Table IV
Modulus of Rupture of A-355.6-G
at Various Temperatures

Specimen number	Test temperature, °F	Modulus of rupture, psi
194	75	91,900
195		86,120
196		80,020
197		97,470
198		82,710
Average		87,640
70	1800	58,000
80		58,000
90		58,000
93		58,000
Average		58,000
79	2000	47,000
81		45,000
86		46,000
87		44,000
Average		45,500
74	2200	43,000
75		45,000
76		53,000
82		41,000
Average		45,500
83	2400	53,000
84		40,000
88		31,000
89		31,000
Average		38,750

A curve showing modulus of rupture versus test temperature is given in Figure 4. It may be noted that the value at 75°F is considerable higher than the 58,000 psi maximum obtained in determining the optimum firing temperature early in the investigation. At present the only interpretation placed upon this change is that the higher strength reflects

a higher degree of development in the technical art of processing the specimens.

Modulus of rupture data for AT-355.6-G and AZ-355.6-G bar specimens result from brief experimentation directed toward learning whether small additions of TiO_2 or ZrO_2 to the basic A-355.6-G composition could increase the wetting and bonding between the Cr-Mo alloy and alumina to a degree which would be reflected in strength tests. Those specimens for which data are given were fired to 3050°F rather than 3150°F, which is considered optimum for A-355.6-G. Strong evidence of overfiring was apparent when the "AT" or "AZ" specimens were fired at the higher temperature. The strength values obtained are given below in Table V, with similar values for control specimens of A-355.6-G.

Table V

Modulus of Rupture

AT-355.6-G and AZ-355.6-G

Designation	Specimen number	Modulus of rupture, psi
A-355.6-G	193	81,500
"	199	66,300
AT-355.6-G	12	69,500
"	13	67,600
AZ-355.6	14	72,600
"	15	66,800

No strong tendency is shown by these limited data, and the question of the effect of the additions is considered unanswered.

In Tables VI and VII the variation of modulus of rupture at 750°F and at 2000°F is shown as related to maturing temperature and metal content of the "AC" series compositions.

Table VI

Modulus of Rupture in psi at 75° for AC Series Specimens

Composition designation	Firing temperature, °F			
	2950	3000	3050	3100
AC-355.6-G	39,500	-	54,800	51,500
	40,300	-	53,500	51,800
AC-373-G	60,300	69,500	36,100	32,000
	75,800	61,900	65,900	27,200
		66,700		
		62,300		
AC-381-G	77,900	74,300	71,500	42,900
	72,700	70,900	68,800	77,300
	75,600			
AC-385-G	19,700	77,600	63,700	37,300
	62,700	66,300	60,000	70,100
	51,800	68,400		
390-G (pure 80Cr-20Mo)	47,600	64,900		
	70,800	60,800		

Table VII

Modulus of Rupture in psi at 2000°F for
"AC" Series Specimens

Composition designation	Firing temperature, °F			
	2950	3000	3050	3100
AC-355.6-G	31,900	-	36,000	38,000
	31,950	-	37,000	43,300
AC-373-G	53,000	63,100	67,100	72,300
	55,700	56,000	66,700	78,500
		63,200		
		59,700		
AC-381-G	88,200	63,800	95,400	96,900
	82,000	98,900	92,000	99,200
		97,200		
AC-385-G	90,800	83,600	88,500	100,000
	96,000	87,800	90,400	88,500
		87,400		
390-G (pure 80Cr-20Mo)	98,800	105,800		
	95,600	105,500		

From the data in Table VI the proper firing temperature appears to be between 3000°F and 3050°F for all compositions. The temperature, 2950°F, is judged to be too low on the basis of considering composition trend jointly with maturing-temperature trend, but the data do not permit a strong conclusion.

The data in Table VII indicate that the higher firing temperatures up to 3100°F favor the 2000°F bending strength. Considerable deformation precedes failure in all cases, and the specimens having the higher metal contents and greater deformability at 2000°F appear to be stronger, but this apparent high strength associated with high metal content is believed to be a function of loading rate and deformability and not a true indication of strength or load carrying ability.

d. Tensile Strength

The tensile strength of A-355.6-G composition is given in Table VIII below and in Figure 5. Tensile strength data were not determined for other compositions except as previously reported for A-16.14-G¹.

Table VIII
Tensile Strength at Various Temperatures

Composition A-355.6-G

Specimen No.	Temperature of test, °F	Tensile strength, psi
32	75	53,280
33	75	52,900
35	1600	40,350
31	1800	28,500
29	2000	25,000
23	2200	18,600
24	2200	31,550
37	2400	9,415

e. Tensile Stress Rupture

Tensile stress rupture properties for the composition A-355.6-G were determined at 1800°F and 2000°F. The results are given in Table 9 below and Figure 6.

Table IX
Tensile Stress Rupture Data
Composition A-355.6-G

Specimen No.	Stress at 1800°F, psi	Time to failure, hrs.
1	18,000	942
2	15,000	1307-no failure
2 reloaded	20,000	872
9	22,000	22
15	25,000	11.6

Specimen No.	Stress at 2000°F, psi	Time to failure, hrs.
11	16,000	1.5
14	15,000	1.9
16	10,000	17.1
19	8,000	31.7
22	7,000	95.9

f. Modulus of Elasticity

The modulus of elasticity was determined using bar specimens of composition A-355.6-G loaded transversely. The bars were supported on a 3-inch span and loaded at the center. The outer fiber stress was calculated from the applied load, and the outer fiber extension was measured by means of Baldwin Locomotive Works SR-4 type A-7 electric strain gages having an 0.25-inch gage length. Completely straight-line stress-strain curves resulted from loading to outer-fiber stresses between 10,000 and 50,000 psi. As a result of three determinations using two specimens and loading at 10,000 psi intervals from 0 to 50,000 psi for each determination, the values 46.8×10^6 , 43.6×10^6 and 44.9×10^6 psi were determined for the modulus of elasticity. It is recognized that these values may be as much as 4% too high because strain was measured over a length and stress was calculated for a point directly beneath the applied load. It was not considered worth while to correct for this effect, since it amounts to less than the difference between specimens and approaches the difference in value for the same specimen in different determinations.

g. Oxidation Resistance

The oxidation behavior of A-355.6-G was determined at 2000°F in the air atmosphere of an electrically heated laboratory furnace. There was no provision for forced air circu-

lation, but vertical door openings and small apertures in the furnace provide a certain stack action and preclude a completely stagnant atmosphere of depleted oxygen content. Results are reported in Table X below in terms of weight gain in grams per square centimeter of surface area for two cylindrical rod specimens.

Table X
Oxidation at 2000°F
Composition A-355.6-G

Elapsed Time, hrs.	Wt. gain, gm/cm ²	
	Specimen No. 1	Specimen No. 2
26	0.00248	0.00274
49	0.00254	0.00283
97	0.00245	0.00279
122	0.00222	0.00276
411	0.00205	0.00260
651	0.00182	0.00251
1011	0.00152	0.00218

These data are shown graphically in Figure 7.

h. Impact Resistance.

No standard impact tests of compositions covered by this report were made. However, it can be stated that bar specimens of composition A-355.6-G can be broken by dropping from a height of approximately four feet onto a concrete floor. In order for fracture to occur, the bar must land perfectly flat on its largest face (0.4 inch x 4 inches). Specimens of higher metal content in the "AC" series are somewhat more resistant to impact, but can be broken by throwing onto a concrete floor so that they strike flat against it.

i. Thermal Shock

Thermal shock data were obtained at the Power Plant Laboratory, WADC, by means of a test procedure which simulates the conditions of burner blow-out in a jet engine operating at altitude and employs nozzle diaphragm blades as test specimens. Thermal shock testing of flame holders was conducted at the National Bureau of Standards by a procedure which consists of cycling the specimens between a burning exhaust stream from a jet engine and a high-velocity air stream. In the test, which was conducted by The Power Plant Laboratory, WADC, a

single cycle involves heating to test temperature (1800°F or 1900°F), holding at this temperature for 1.5 minutes, and then turning off the fuel and allowing high velocity air to continue flowing over the test blade for 30 seconds. Cycling is continued until failure by fracture or until 1000 cycles have been completed.

In a test which was conducted on flame holder specimens at the National Bureau of Standards, the specimen was held between water-cooled copper members inserted into the hollow opening of the flame holder. It was plunged into the combustion stream which had a maximum theoretical flame temperature of 3500° and a mass flow of 15 lbs/sq ft/sec, and held until a brightness temperature (optical pyrometer measurement) of 2100°F had been reached. Within one second it was withdrawn and plunged into a 125°F stream of air having the same mass flow. This treatment will fail fused quartz, and certain other materials rated excellent in thermal shock resistance, in one cycle. The cycle is repeated thirty times unless fracture failure occurs.

Table XI below contains the results of testing certain A-16.14-G and A-355.6-G nozzle blades.

Table XI
Thermal Shock Endurance of Nozzle
Diaphragm Blades

Composition and O.S.U. No.	Design	WADC No.	Temperature, °F	Cycles
Composition A-16.14-G				
12	J-47	48	1800	320
20	"	?	"	620
2	J-35 Hollow	110	1900	10
3	J-35	65	"	350
4	"	66	"	320
5	"	67	"	80
6	"	68	"	140
7	"	111	"	510
Composition A-355.6-G				
1	J-35	79	1900	990
2	"	80	"	1020**
4	"	81	"	120***
5	J-35 Hollow	112	"	1000
6	J-35	113	"	250
7	"	114	"	1000
8	"	115	"	1000

*Airfoil cross-section.

**Test stopped. Did not fail. No cracks or signs of fracture.

*** Highest degree of Al₂O₃ segregation noted in over 100 metallographic examinations of A-355.6-G specimens of various rod, bar, and blade types.

The thermal-shock testing of four A-16.14-G flame-holder specimens by the National Bureau of Standards as described above resulted in all four specimens withstanding 30 cycles without cracking or fracture. Oxidation resistance appeared adequate. The flat back was removed from two of the flame holders before testing by cutting with a band saw. Four A-355.6-G specimens have also been submitted for test, but data are not available for reporting at this time.

j. Thermal Expansion

The thermal expansion of Cr, of 80Cr-20Mo alloy, and of A-355.6-G, in which 80Cr-20Mo is the metal phase, are presented for comparison in Figure 8.

The data on which the curves are based are given below in Tables XII, XIII, and XIV.

Table XII
Thermal Expansion of A-355.6-G

Run A		Run B		Run C	
Temp., °F	Length Change, %	Temp., °F	Length Change, %	Temp., °F	Length Change, %
90	—	90	—	80	—
220	0.027	900	0.280	305	0.050
925	0.382	1400	0.567	395	0.082
1350	0.530	1930	0.966	480	0.111
1840	0.864	1690	0.770	650	0.173
2110	1.053	1125	0.427	690	0.192
2440	1.400	90	0.014	740	0.215
2200	1.209			760	0.223
2055	1.110			975	0.318
1900	0.967			1030	0.351
1690	0.828			1480	0.617
1550	0.750			1600	0.695
1460	0.659			1700	0.770
1280	0.560			1910	0.947
1070	0.471			2035	1.073
945	0.429			2120	1.133
815	0.355			1970	0.972
640	0.299			1845	0.883
295	0.207			1685	0.762
120	0.196			1225	0.470
				880	0.299
				760	0.238
				680	0.214
				530	0.154
				350	0.093
				175	0.032
				80	0.001

Table XIII
Thermal Expansion of Cr

Temp., °F	Length Change, %	Temp., °F	Length Change, %
75	—	80	—
145	0.034	95	0.003
180	0.043	150	0.028
250	0.068	235	0.061
375	0.111	295	0.082
520	0.180	355	0.111
595	0.220	450	0.148
720	0.285	690	0.266
820	0.338	795	0.330
925	0.398	895	0.386
1010	0.444	1065	0.482
1115	0.504	1205	0.570
1280	0.610	1355	0.665
1355	0.668	1505	0.776
1440	0.737	1560	0.815
1600	0.846	1748	0.967
1725	0.933	1798	1.010
1925	1.102	1905	1.101
2035	1.227	2020	1.219
2135	1.353	1915	1.120
2285	1.547	1805	1.025
2400	1.733	1645	0.892
2245	1.501	1485	0.765
2125	1.361	1320	0.657
2025	1.250	1160	0.554
1610	0.888	1000	0.457
1535	0.852	880	0.384
1395	0.740	575	0.229
1290	0.673	485	0.185
1135	0.577	365	0.133
980	0.481	285	0.100
740	0.358	180	0.055
385	0.184	110	0.025
245	0.127	80	0.011
80	0.040		

Table XIV
Thermal Expansion of 80Cr-20Mo

Temp., °F	Length Change, %	Temp., °F	Length Change, %
80		80	
210	0.051	200	0.048
270	0.092	290	0.089
350	0.131	440	0.159
460	0.186	660	0.272
560	0.244	840	0.369
695	0.317	1010	0.458
810	0.410	1250	0.605
925	0.484	1460	0.743
1050	0.585	1630	0.862
1310	0.857	1790	0.990
1435	0.969	Test interrupted	
1590	1.191		
1710	1.341		
1910	1.567		
2040	1.648		
2220	1.816		
1940	1.564		
1810	1.453		
1670	1.349		
1540	1.254		
1360	1.134		
1180	1.007		
1020	0.917		
760	0.776		
610	0.695		
450	0.620		
350	0.578		
80	0.458		

All specimens display some permanent expansion which may be real or apparent. Large apparent permanent elongation which is observed during the first run for a particular set-up is believed to be caused by deformations of the wire references used in making thermal length change measurements. Reference to Figure 9, which shows the equipment used in making these thermal expansion measurements, will make this clear. Weighted reference wires attached to the ends of the specimens drop through a slot in the bottom of the furnace. Micrometer filars in a pair of telescopes are used to measure the horizontal distance between the wires to an accuracy of 0.001 mm.

If the wires are not strain free at the start of the run, but undergo strain release during the run, erratic results are obtained. These always take the form of apparent permanent elongation, and are associated with an initial set-up rather than an initial determination on a particular specimen. In light of these observations, the foregoing data were interpreted as follows:

- (1) The initial heating portion of a thermal expansion determination for a particular set up was considered to be unreliable, but the cooling curve was considered to yield useful data.
- (2) The heating and cooling portions of curves resulting from repeat runs involving a particular specimen and set up were considered to be equally valid.
- (3) Because specimen temperature lags measured temperature during both heating and cooling portions of the cycle, and since this lag is greater at low temperatures than at high temperatures for a given rate of furnace temperature change, the curve obtained during furnace cooling should lie above the curve obtained on heating, and the spread should increase as temperature decreases. This pattern characterized repeat runs and the mean curve lying between those obtained on heating and cooling was taken as the true curve.

By interpreting the data in accordance with these principles curves (1), (2), and (3) in Figure 8 were drawn as those best representing the data.

Curve (4), Figure 8 is for Al_2O_3 . It results from a study which anticipated the desirability of knowing the thermal expansion of Al_2O_3 and the effect on thermal expansion of Al_2O_3 caused by Cr_2O_3 in solid solution. Specimens approximately 20cm long were prepared containing 80% Al_2O_3 -20% Cr_2O_3 , 90% Al_2O_3 -10% Cr_2O_3 , 95% Al_2O_3 -5% Cr_2O_3 , and 100% Al_2O_3 . These were sintered at 3000°F in a gas-fired furnace. They were somewhat porous, and there is some doubt concerning the completeness of solid solution of the two oxides. However, the ruby color becomes progressively darker with increasing Cr_2O_3 content, and on the basis of ruby color intensity there is little doubt that the Cr_2O_3 in solid solution is at least one third of that in the initial mixture. The specimens containing 100% Al_2O_3 , 90% Al_2O_3 -10% Cr_2O_3 , and 80% Al_2O_3 -20% Cr_2O_3 were employed in thermal expansion determinations up to 1470°F using a silica-tube dilatometer. Only the curve for the 100% Al_2O_3 specimen is plotted in Figure 8, because there was no significant difference in thermal expansion found for the different compositions. This is shown by the data in Table XV below.

Table XV

Thermal Expansion of Al_2O_3 and Al_2O_3 plus Cr_2O_3

100% Al_2O_3		90% Al_2O_3 -10% Cr_2O_3		80% Al_2O_3 -20% Cr_2O_3	
Temp., °F	Length Change, %	Temp., °F	Length Change, %	Temp., °F	Length Change, %
70	0	87	0	77	0
250	0.045	176	0.018	300	0.064
320	0.076	290	0.062	430	0.115
392	0.095	428	0.118	470	0.126
460	0.115	530	0.157	600	0.184
510	0.149	590	0.182	680	0.212
572	0.170	690	0.217	780	0.256
626	0.191	788	0.266	895	0.310
752	0.244	854	0.296	1040	0.381
932	0.326	980	0.370	1130	0.425
1040	0.378	1054	0.387	1240	0.479
1130	0.416	1170	0.446	1290	0.501
1220	0.460	1252	0.489	1395	0.555
1350	0.528	1310	0.512	1455	0.585
1436	0.564	1420	0.564	1530	0.631
1472	0.592	1450	0.583	1040	0.391
1436	0.579	1472	0.593	878	0.316
1418	0.567			79	0.005
1348	0.535				
1292	0.507				
1215	0.465				
1154	0.437				
1120	0.430				
1000	0.366				
878	0.311				
745	0.252				
108	0.029				
99	0.023				

It is noteworthy that the thermal expansion of A-355.6-G falls below that measured for Al_2O_3 and $(\text{Al}, \text{Cr})_2\text{O}_3$, and this will be considered further in the DISCUSSION section of this report.

k. Metallography

Approximately 100 metallographic examinations of various

specimens of A-355.6-G or related compositions have been made during the course of this study in order to observe structural properties. Of these, four are considered to be worth incorporating in this report to show the sound structure and phase distribution generally present in A-355.6-G specimens and certain departures from this structure which have been observed.

Figure 10 shows a typical good microstructure of A-355.6-G observed in random areas of bar, rod, and blade specimens.

Figure 11 shows a segregation of the metal phase into globules in A-355.6-G specimens which were composed of alumina and 80Cr-20Mo alloy which had been separately milled for 50 hours by the same ball milling technique employed in the final batch milling operation. The cause for the globuliferous structure is not definitely known, but is assumed to be associated with additional milling impurity pickup, since the additional milling of the alloy is the single known difference in processing technique. The specimens were fired together.

Figure 13 shows the most extreme condition of Al_2O_3 segregation observed in any specimen of the A-355.6-G composition. It is the structure of the nozzle diaphragm blade which failed after 120 cycles in the WADC thermal shock test described in Part g above.

Figure 12 shows a condition of segregation in the A-355.6-G composition, observed in rod specimens used for stress-rupture testing.

1. Hardness

A single A-355.6-G specimen, Blade Number 1 of the J-35 design, was tested for hardness using a Vickers-Armstrongs Hardness Tester. With a 20-kilogram load and a 2/3 inch objective, an average hardness number from seven indentations was 689. Using a 50-kilogram load and a 2/3 inch objective, a hardness number of 698 resulted from two indentations. This agreement indicates the right range of test conditions. Thus a VPN hardness of 690-700 or a Rockwell C (from Vickers-Rockwell Table) hardness of 57-58 is taken as representative of the gross hardness of the A-355.6-G body.

m. X-ray

X-ray techniques were used to determine the completeness of solid solution in the formation of the 80Cr-20Mo alloy. Early in the investigation it was learned that 3050°F produced complete diffusion alloying. All subsequent samples from fired specimens show complete solid solution as would be expected from their heat-treating history and the phase diagram².

X-ray studies were also employed to determine the unit cell size of the corundum phase in the A-355.6-G cermets. This was done because Cr_2O_3 dissolved in $\alpha\text{-Al}_2\text{O}_3$ produces an expansion of the unit cell, and knowledge of the amount of expansion furnishes insight into the amount of Cr oxidized to Cr_2O_3 and dissolved in the Al_2O_3 during firing. Vegard's law is considered applicable in that the edge length of the unit rhombohedron, a_0 , can be taken as indicative of the cationic composition of the corundum phase, and the angle α differs so little between the unit rhombohedrons for Al_2O_3 and Cr_2O_3 that changes in its value can be disregarded for intermediate solid solutions. Therefore, the ratio of the difference between a_0 for the solid solution and a_0 for Al_2O_3 to the difference between a_0 for Cr_2O_3 and a_0 for Al_2O_3 is the fraction of Cr_2O_3 in the solid solution.

The a_0 determinations were made from patterns resulting from the use of filtered Cr radiation. The four back reflection lines bearing the rhombohedral indices 433, 432, 202, and 311 were used in the unit cell size determination by plotting the a_0 values calculated from each of these lines versus the respective $\cos^2\theta$ values and extrapolating to the a_0 value for $\cos^2\theta=0$. The a_0 value corresponding to $\cos^2\theta=0$ is used as the true edge dimension of the unit rhombohedron.

Following this procedure and assuming that departure from the unit cell size of $\alpha\text{-Al}_2\text{O}_3$ is entirely due to solution of Cr_2O_3 , the following amounts of solid solution were estimated:

<u>Rod specimen No.</u>	<u>Dissolved Cr_2O_3, %</u>
1	2.4
2	3.1
9	3.6
11	3.4
14	2.6
15	2.2
16	2.6

The fact that these values are significantly lower than those observed for A-16.14-G¹ raises the question of whether or not Mo is also dissolved, contracting the unit cell and decreasing the apparent Cr_2O_3 solution, and whether less Cr_2O_3 is formed and dissolved when the Cr source is 80Cr-20Mo alloy than when it is pure Cr metal. For the particular specimens sampled, the firing atmosphere condition is believed to be quite similar to that used in firing the earlier A-16.14-G specimens, although dew-point measuring equipment was not used to assure this fact. Attempts to answer the question of Mo solid solution and to check independently the amount of Cr_2O_3 dissolved, by acid leaching the metal and chemically analyzing the corundum residue, were unsuccessful in that it was found impossible to remove the metal completely by leaching. Microscopic examination of the residue revealed that corundum crystals as small as 10

microns contained occluded metal particles.

VIII DISCUSSION

A certain amount of discussion has been immediately associated with description of certain procedures, tests, or results presented in earlier sections of this report. This was done where it was considered preferable for the sake of clarity to explain or interpret in conjunction with the presentation of factual information. In this regard a discussion of firing atmosphere quality is included under the FIRING section, and the interpretations of thermal expansion data and certain X-ray and metallographic observations are included under PROPERTY EVALUATIONS. Further discussion will be devoted to the composition A-355.6-G, its modifications, and the composition A-16.14-G as a flame-holder material.

Density

The measured density of A-355.6-G is almost exactly that which would be predicted by regarding it as a completely dense mechanical mixture of the two phases. Despite the Mo content, A-355.6-G is no higher in specific gravity than A-16.14-G, because it contains almost exactly equal volume proportions of metal and Al_2O_3 , whereas A-16.14-G contains somewhat more than half pure Cr metal by volume. In the prior development of A-16.14-G this Cr content was found necessary to provide adequate thermal shock resistance. An improved thermal shock resistance has been obtained in A-355.6-G with a lower volume content of a heavier alloy. The differences in specific gravity and volume proportions of metal were such that no concession in the direction of higher specific gravity was necessary in improving thermal shock resistance.

Mechanical Properties

The strength properties of A-355.6-G are good in all types of evaluation - modulus of rupture, tensile tests, and stress-rupture tests - up to 1800°F. At 2000°F the stress sustaining ability appears to fall rapidly as shown by the extrapolated 1000-hour life of 4000 psi. At 1800°F the 1000-hour life is 19,000 psi from Figure 6. This value is well established experimentally by actual specimen failures following 800 to 1000 hours of test. The curve showing tensile strength as a function of temperature in Figure 5 does not indicate a sharp decrease in strength over the temperature interval between 1800°F and 2000°F. Therefore, the stress-rupture behavior indicates a time-dependent effect at 2000°F rather than an effect which is singularly temperature dependent.

That this effect may depend upon oxidation behavior is shown by certain fractures of stress-rupture specimens on which an oxidation tint appears in a roughly triangular pattern with one apex at or near the rod axis. This pattern could result from crack propagation where the crack originates at the surface, deepens toward the center of the rod, and enlarges circumferentially. This observation is not confined to 2000°F tests, but also applies to specimens that failed at 1800°F. It may be that the sharp difference in 2000°F stress-rupture behavior compared to 1800°F behavior is due to stress-corrosion of an oxidation type, and this may be the mechanism of specimen failure in all cases.

As reported earlier in a progress report submitted under this contract, one rod specimen (number 2) displayed a true strain at the minimum section of the neck of 0.024. This occurred during 942 hours in the test at 1800°F and 18,000 psi. Although this manifestation of plastic deformation was not confirmed as a result of checking all other specimens tested in stress rupture, there is nevertheless considerable confidence in this single result because it is based on initial diameter measurements before the initial test and before the reload test: these were identical. The final diameter measurements were carefully checked, and a diameter decrease of 0.003 inch was determined. The same micrometer was used in making all measurements. This results in the reported true strain of 0.024 at the minimum section. Although this observation could result from error, it is presently interpreted as a unique behavior for which no ready explanation exists.

The average modulus of elasticity for A-355.6-G has been determined as 45×10^6 . That previously determined for A-16.14-G is 47×10^6 , and this is associated with a higher volume content of a metal of presumably lower modulus of elasticity. Stated differently, 80Cr-20Mo would be expected to have a modulus of elasticity higher than that of pure Cr, which is approximately 35×10^6 . From these facts it is apparent that in this composition range the hard phase places considerable restriction on the manner in which the metal can be strained in an elastic way. This is contrasted to other two phase mixtures, in which the hard phase is discontinuous in the form of discrete particles and is present in smaller amounts, so that the modulus of elasticity of the composite is practically the same as that of the matrix phase. It is also apparent that the elastic behavior of alumina base cermets is insensitive to the amount of metal present in this composition range, and also to minor changes in the modulus of elasticity of the metal phase, otherwise A-355.6-G, should have a slightly higher modulus of elasticity than A-16.14-G instead of a slightly lower one. Alternatively, if this range of values is considered to be within that of experimental error, it follows that the modulus of elasticity is not notably effected by the difference of 8% by volume of metal or by the difference in character of Cr and an 80Cr-20Mo solid solution alloy.

Modifications

Modifications of the A-355.6-G body were studied for the purpose of gaining insight into possible ways of improving mechanical properties. In those brief studies only modulus of rupture was consistently evaluated. Impact resistance level was determined in certain instances by the crude method of dropping or throwing bar specimens on to a concrete floor.

The AT-355.6-G bar specimens and the AZ-355.6-G bar specimens are A-355.6-G plus 1 percent TiO_2 and 1 percent ZrO_2 respectively. In an initial sintering operation these specimens were overfired. In the second firing for which data are given, there was no significant difference between the specimens of the modified composition and those of A-355.6-G fired at the same time for comparison. In view of the brevity of the study, the question of whether improved mechanical properties are attainable through such additions is considered undertermined.

To study the effect of phase proportions on mechanical properties, compositions of alumina and various amounts of 80Cr-20Mo alloy were prepared. It was thought desirable to use a very fine alumina in the batch in order to insure a good distribution of this phase in those bodies containing alumina in small quantities. Therefore, calcined aluminum hydrate was employed. Compositions varied from 50% to 95% 80Cr-20Mo alloy by volume and are designated as "AC" series specimens in the PROPERTY EVALUATION section of this report. All specimens (including 100 percent 80Cr-20Mo alloy) in the series are sufficiently brittle at room temperature to be broken by throwing flat on a concrete floor. However, in modulus of rupture testing at 2000°F, plastic deformation precedes fracture in those specimens containing 85% or more metal. This was observed during test and is further indicated by the fact that high-metal specimens appear to be stronger at 2000°F than at room temperature. As indicated above, no outstanding improvement in impact resistance resulted from the study, because a certain impact sensitivity is characteristic of the metal component.

Thermal Properties

The thermal shock resistance of A-355.6-G is excellent, as indicated by the consistent ability of nozzle diaphragm blades to withstand cycling in the WADC Power Plant Laboratory test operated at 1900°F. Of the eight blade specimens made from this composition, seven were submitted for test. From this group, four specimens withstood 1000 cycles or more, one withstood 990, one failed at 250 cycles for undetermined reasons, and one failed at 120 cycles, apparently because of an unusually poor structure (Figure 13). If this last specimen is eliminated because of its poor structure, five out of six specimens withstood approximately 1000 cycles (one withstood 990, another 1020) from 1900°F. Inherent merit of the composition is further indicated by the fact that these were the

initial specimens of this type fabricated from the A-355.6-G body, and all of the blades were solid except one.

The data on thermal shock behavior of A-16.14-G in the form of flame-holders, obtained by the National Bureau of Standards, Refractories Section, indicate excellent thermal shock performance, although previous results of nozzle diaphragm blade testing¹ had placed this composition in a marginal category. Present data should be considered as supplementary to the earlier information.

The thermal expansion of A-355.6-G was found to be less than that measured for Al_2O_3 between 1300°F and room temperature. This type of behavior has been noted previously for Cr- Al_2O_3 bodies¹, but was discounted in terms of possible effects of milling impurity pick-up and the previously unknown effect attributable to dissolved Cr_2O_3 on thermal expansion of Al_2O_3 . This latter possible effect is now known to be negligible with regard to the order of magnitude by which the thermal expansion of the cermet differs from the average thermal expansion of the phases Al_2O_3 and 80Cr-20Mo. The depression in thermal expansion is also much greater than that which could be ascribed to milling impurities. Tungsten is the only impurity which could lower the thermal expansion of the metal phase, and it is not reasonable to expect 2-3 % W (by weight) to have a greater effect than 20% Mo (by weight), and the effect of this proportion of Mo can be seen to be small by comparing curves 1 and 2 in Figure 8. Therefore, the depression effect is real, but previous tentative explanations are inadequate.

The correct explanation for this behavior is believed to be as follows:

(1) The alloy has the greater thermal expansion and therefore tends to contract more than Al_2O_3 upon cooling the cermet from the maturing temperature.

(2) At room temperature the metal resides in triaxial tension, the Al_2O_3 in triaxial compression. To visualize this imagine a sphere of relatively high-expanding metal perfectly bonded to a rather thick surrounding spherical shell of relatively low-expanding Al_2O_3 . Further imagine a stress-free state at some elevated temperature. If the assembly is cooled the metal becomes stressed in triaxial tension, the Al_2O_3 shell in tangential biaxial compression plus decreasing tension radially from the interface outward toward the surface. If the picture is reversed and an Al_2O_3 sphere is surrounded by a thick metal shell, stress-free at an elevated temperature, and this is cooled, it is seen that the Al_2O_3 is placed under triaxial compressive stress and the metal in biaxial tensile stress tangentially plus decreasing compressive stress from the interface to the surface. The cermet body at least approximates a mixture of such spheres in which the metal is predominantly in triaxial tensile stress while the alumina is predominately in triaxial

compression.

(3) The effect of reheating the cermet in which the phases are under stress is to relax the stresses between the phases, in addition to producing thermal length change. If, for example, an elastic elongation of 0.001 inch is placed in a specimen by a fixed holding device, the specimen will not expand until it has undergone a temperature change which will produce 0.001 inch of thermal length change. If the holding device also expands with increasing temperature, but at a slower rate than the specimen, the effect will be to require a greater temperature interval to produce a stress-free condition, or a condition of stress reversal in the holder-specimen assembly.

Consideration of the stressed condition in which the body is believed to reside at room temperature, in the manner outlined above, explains the thermal expansion behavior observed. It also is consistent with the modulus of elasticity measurements, which could not be at the high level observed if the two phases were not intimately bonded into an association which makes each phase effective in transmitting a stress to the other.

The rate of oxidation of A-355.6-G at 2000°F is comparatively rapid for approximately 50 hours, during which time an oxidation weight gain of 2.5 to 2.8 mg/cm² occurs. This is followed by a weight loss ranging between 0.5 mg/cm² and 1.0 mg/cm² during the following 1000 hours at 2000°F. This represents a slightly higher initial weight gain and a slightly faster rate of weight loss than that which was observed for A-16.14-G¹. The maximum gain in weight is acquired in less elapsed time with A-355.6-G than with A-16.14-G. These results are to be expected in a comparison between a cermet containing Cr and one containing 80Cr-20Mo in approximately equivalent volume proportions. However, the effect of the Mo is slight, and the oxidation weight gain, oxidation weight loss, and the rates at which these processes occur at 2000°F are only slightly higher for the Mo-bearing cermet. There is no evidence of detrimental oxidation effect (such as preferential oxidation) due to Mo unless it is significant in explaining the mechanism of stress-rupture failure at 2000°F as tentatively suggested above.

The thermal shock resistance of flame holders composed of A-16.14-G is somewhat better than that which might have been anticipated on the basis of performance of A-16.14-G as nozzle diaphragm blades¹. A-355.6-G flame holders, now in test, should prove to be still better. The flame holder problem includes oxidation corrosion, attachment, and moderate stress aspects, in addition to severe thermal shock. Therefore, these oxide-base cermets may prove to be useful in its solution, for they are adequate with regard to physical properties and lend themselves to simple mounting procedures.

CONCLUSIONS

1. Usefulness in high-stress service to 1800°F is indicated for A-355.6-G by observed oxidation resistance, stress rupture behavior, and thermal shock resistance.

2. Usefulness in moderate stress service to 2000°F and higher is indicated for A-355.6-G by the same properties listed above.

3. Consistently pore-free bodies can be sintered in the A-355.6-G composition.

4. The density of 5.8 to 5.9 observed for A-355.6-G offers a weight advantage and a stress advantage in centrifugally stressed parts, when compared to alloys.

5. The practicability of fabricating a strong join between the A-355.6-G body and other oxide-base cermet compositions or metals has been demonstrated.

6. The effect of ZrO_2 and TiO_2 additions to the A-355.6-G body has not been demonstrated.

7. The effect on mechanical properties of varying the proportions of 80Cr-20Mo alloy and Al_2O_3 in oxide base cermets containing only these two phases is obscured by the brittle characteristics of the alloy.

8. The thermal expansion behavior of A-355.6-G indicates that the metal and Al_2O_3 phases stress each other so as to lower the thermal expansion below the average of the two phases and below that of the lower expanding phase over a range of temperatures up to approximately 1300°F.

9. The physical properties of A-16.14-G appear to be adequate for flame holder applications, and the body lends itself to relatively simple attachment practices.

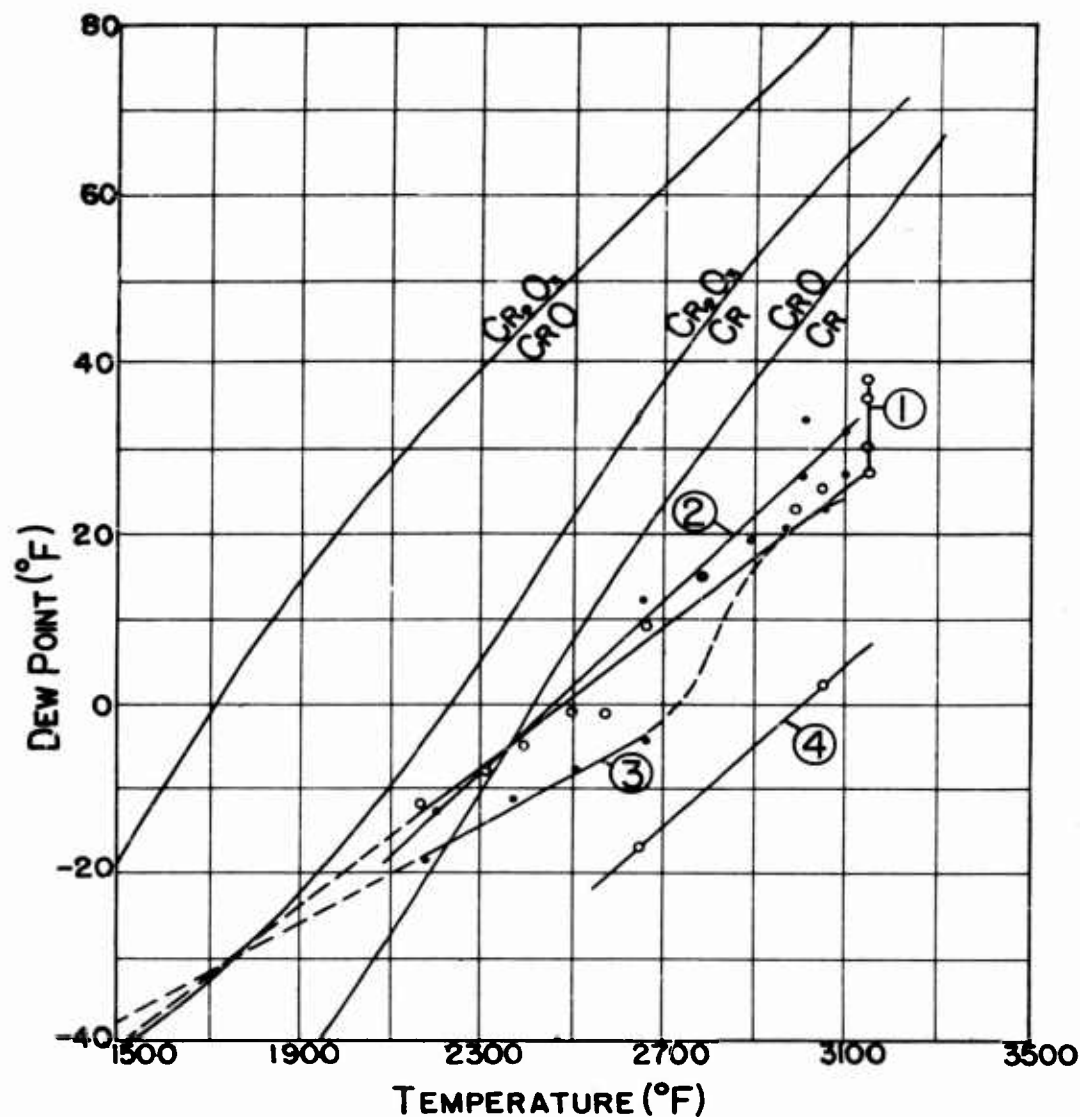
REFERENCES

1. Shevlin, T.S. Development, Properties and Investigation of a Cermet Containing 28% Alumina and 72% Chromium. Wright Air Development Center Technical Report 53-17, December 1952.
2. Sykes, W.P. Metals Handbook (Taylor Lyman, Editor). American Society for Metals, Cleveland, Ohio, 1948, p 1194
3. Parke, R.M. and Bens, F.P. Chromium-Base Alloys. American Society for Testing Materials Symposium on Materials for Gas Turbines, 1946, pp 80-98
4. Shevlin, T.S. The Ohio State University Research Foundation Report No. 29 (1947). AF Contract No. W33-038-ac-14217
5. Shevlin, T.S. The Ohio State University Research Foundation Report No. 34 (1947). AF Contract No. W33-038-ac-14217
6. Leslie, W.C. The Ohio State University Research Foundation Report No. 55(1949). AF Contract No. W33-038-ac-14217.
7. Parke, R.M. and Bens, F.P. Chromium-Base Alloys. A.S.T.M. Symposium on Materials for Gas Turbines, pp 80-98 (1946)
8. Blackburn, A.R., Shevlin, T.S., and Lowers, H.R. Fundamental Study and Equipment for Sintering and Testing of Cermet Bodies I-III. Journal of the American Ceramic Society. Volume 32, 1949, (3) p 91
9. Shevlin, T.S. and Blackburn, A.R. Fundamental Study and Equipment for Sintering and Testing of Cermet Bodies IV. Journal of the American Ceramic Society. Volume 32, 1949, p 363.
10. Maier, C.G. Sponge Chromium. Bureau of Mines Bulletin No. 436, 1942, p 17.



Fig. 1. Forming accessories and flame holders.
Left, steel core. Left center, plastisol casing.
Right center, green flame-holder. Right, fired
flame-holder.

OXIDATION-REDUCTION OF CHROMIUM OXIDES RELATED TO DEW POINT AND FIRING TEMPERATURE



1. ° LARGE MOLYBDENUM FURNACE
2. ° SMALL MOLYBDENUM FURNACE-AS REBUILT
3. ° LARGE MOLYBDENUM FURNACE
4. ° SMALL MOLYBDENUM FURNACE-AFTER CONTINUED USE

FIG.2

POROSITY AND MODULUS OF RUPTURE
VERSUS
FIRING TEMPERATURE
FOR COMPOSITION A-355.6-G

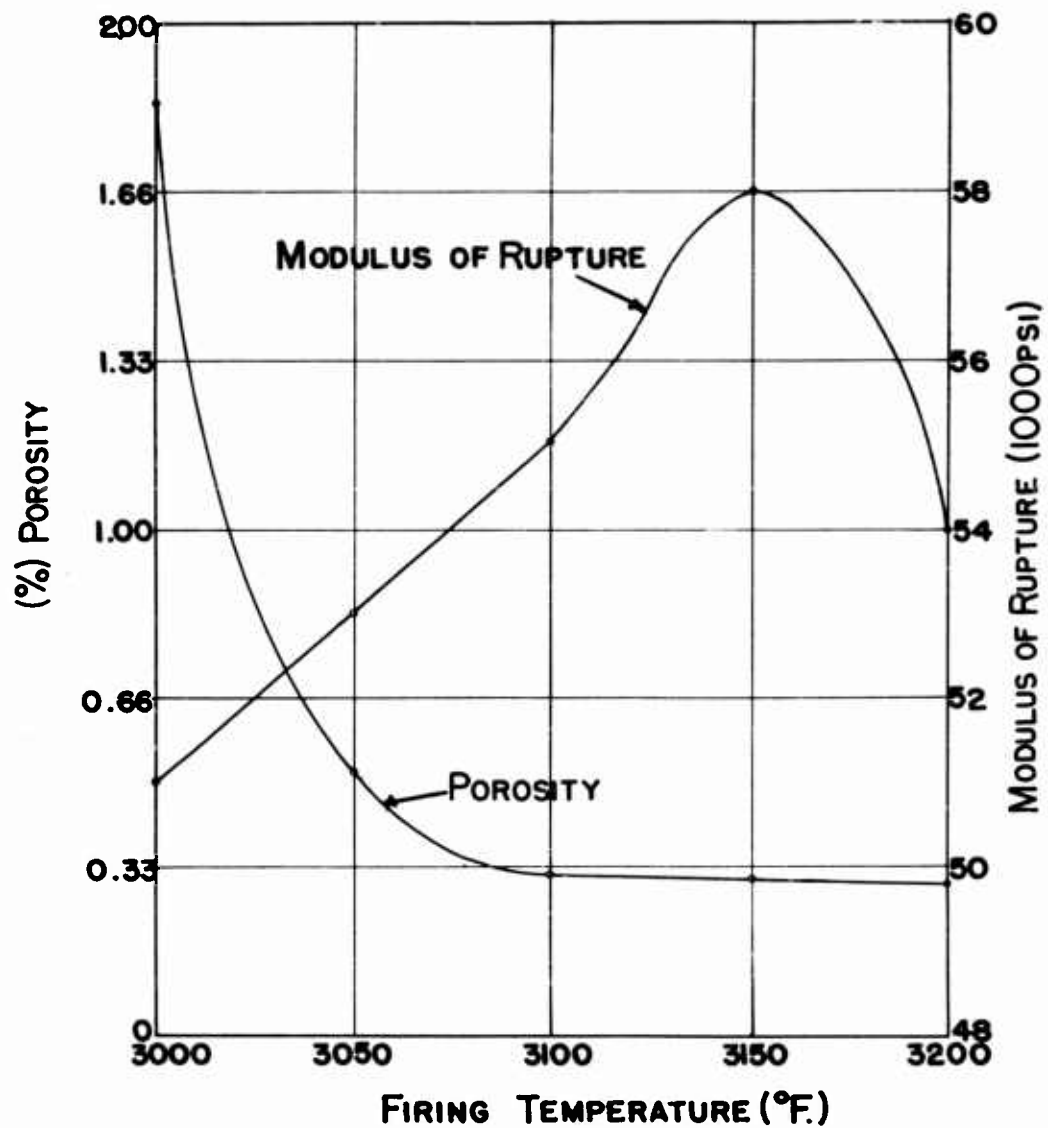


FIG. 3

MODULUS OF RUPTURE
VERSUS
TEST TEMPERATURE
FOR COMPOSITION A-355.6-G

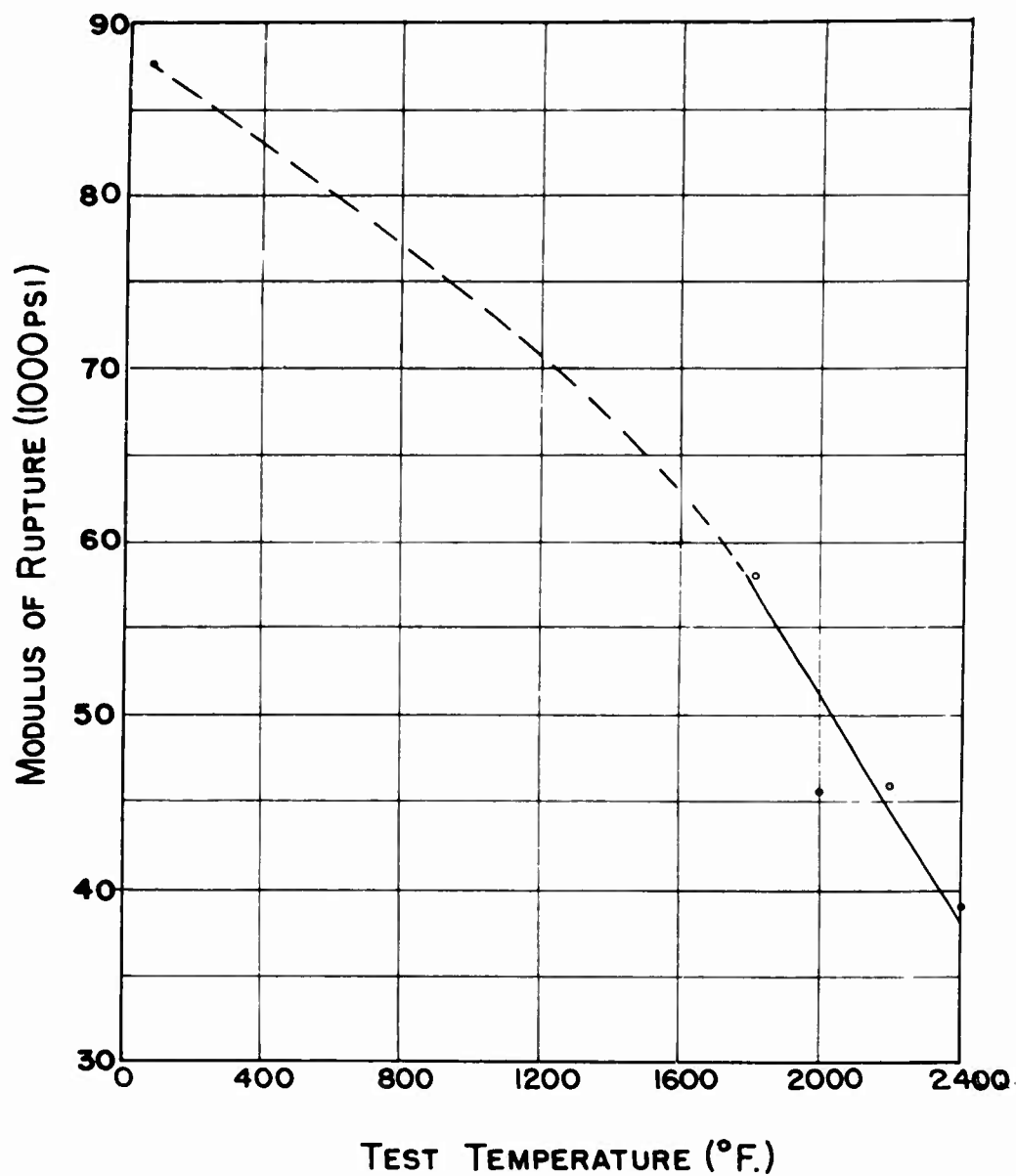


FIG. 4

TENSILE STRENGTH VERSUS TEST TEMPERATURE
FOR BODY A-355.6-G

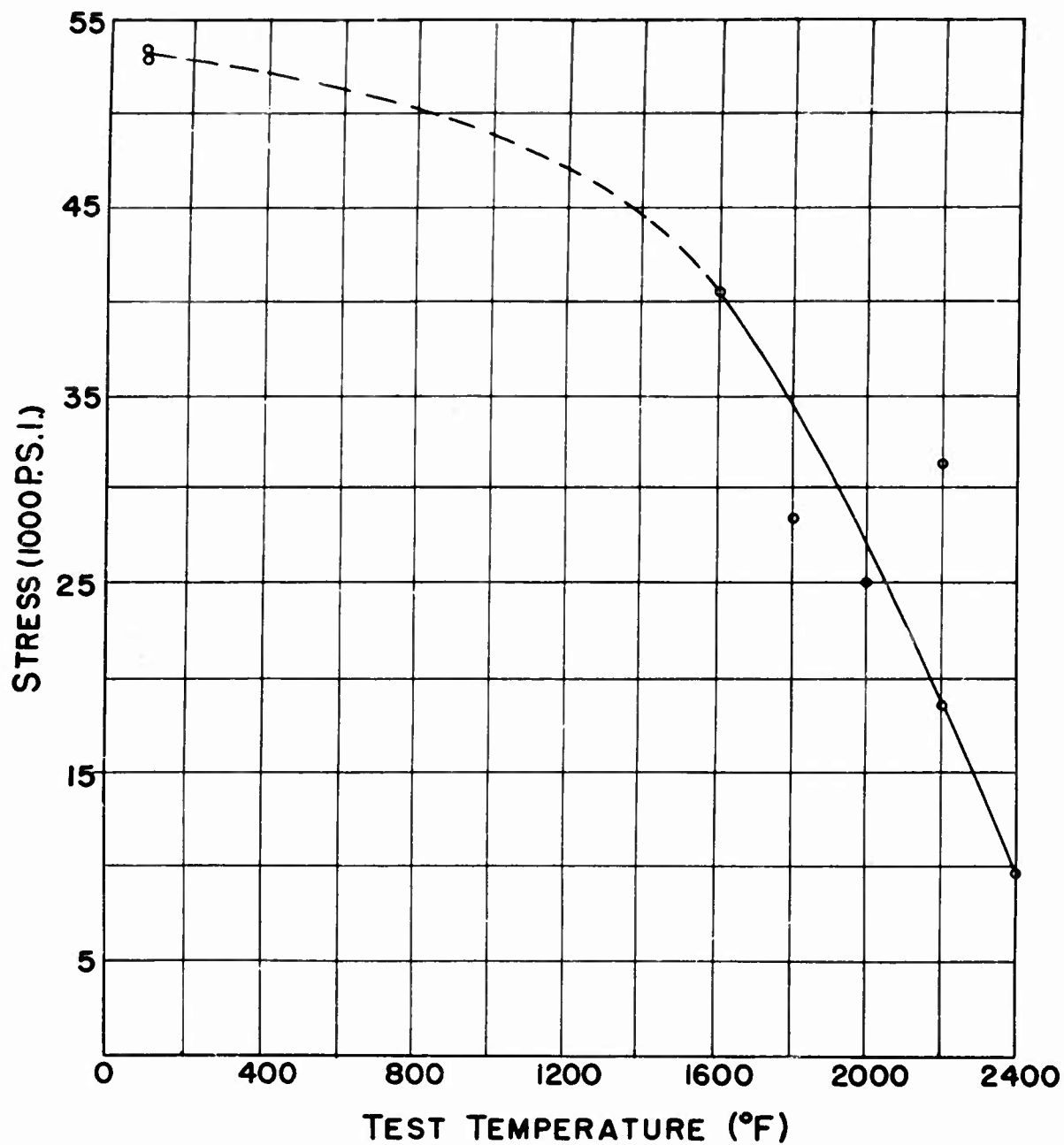
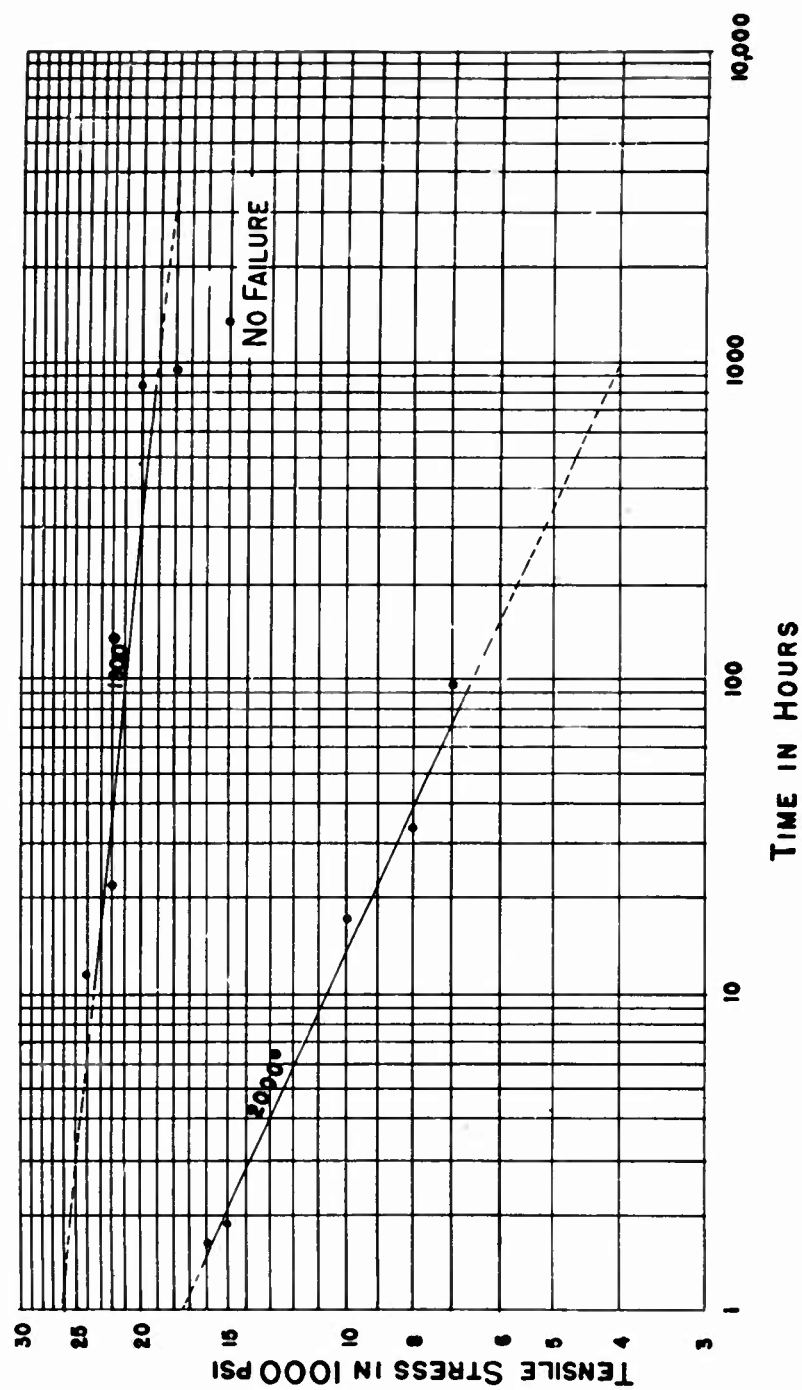


FIG. 5

STRESS RUPTURE IN TENSION FOR COMPOSITION A-3556-G



OXIDATION OF BODY A-355.6-G AT 2000 °F

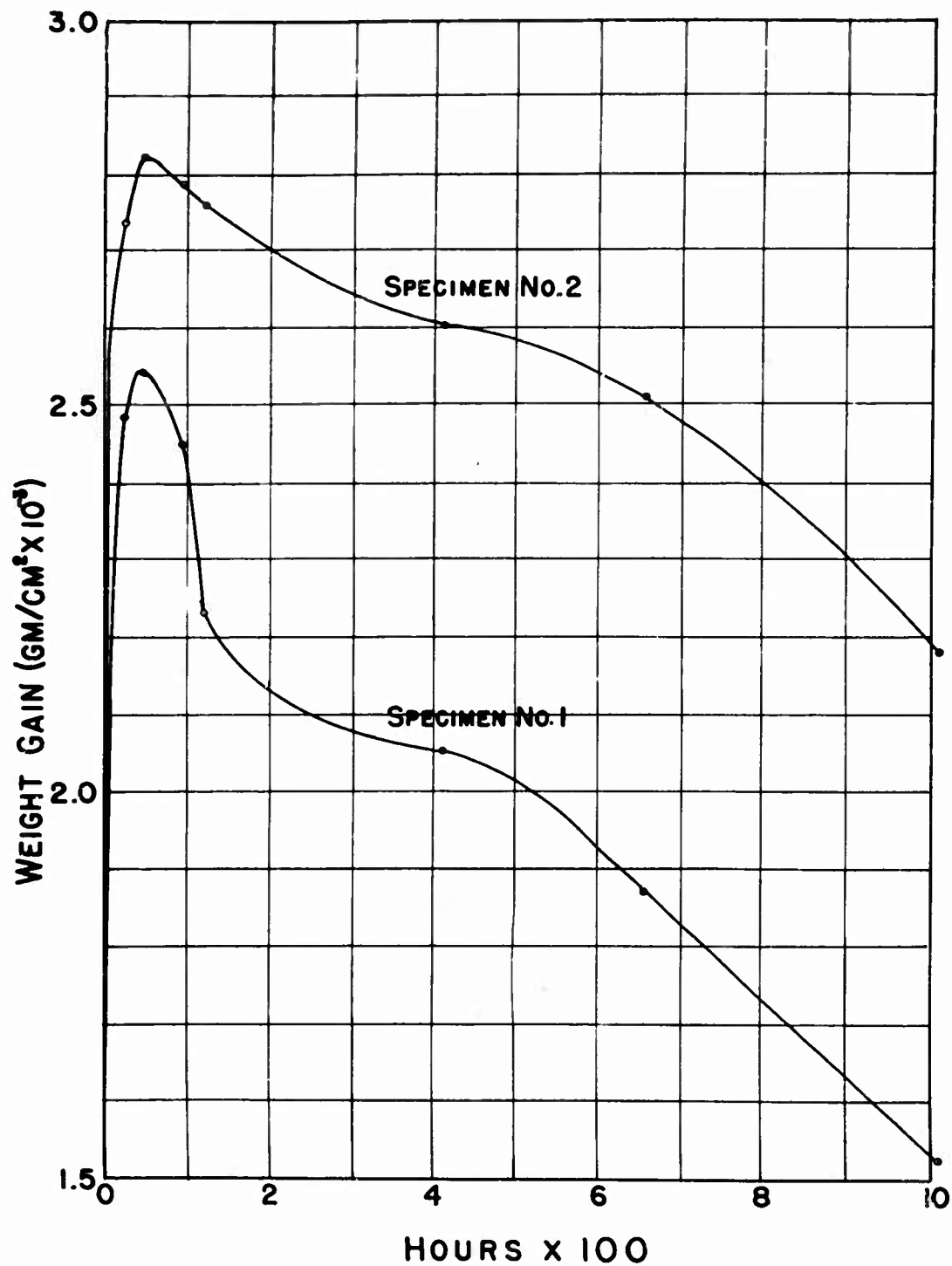


FIG. 7

THERMAL EXPANSION DATA

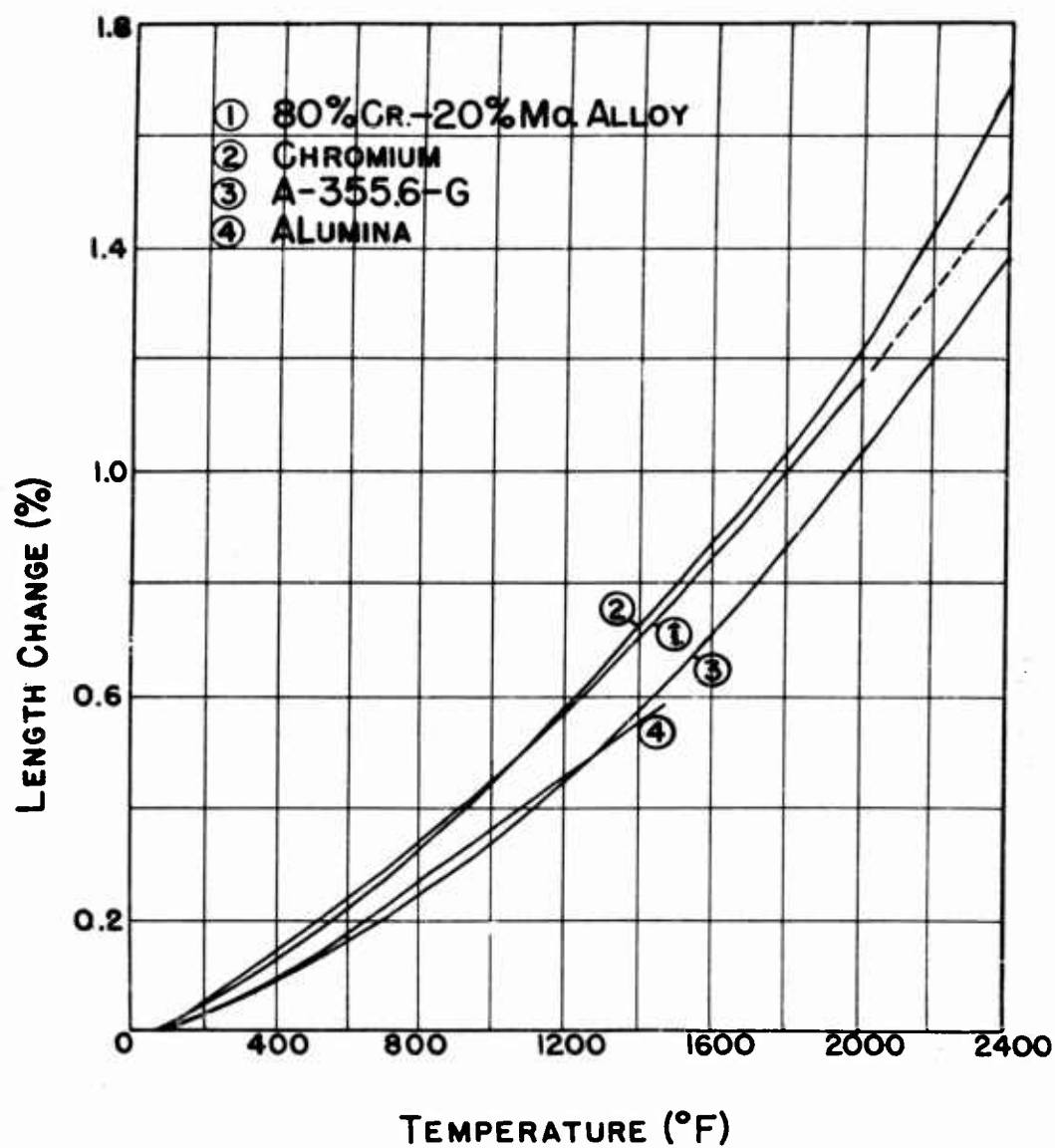


FIG.8

THERMAL EXPANSION FURNACE AND REFERENCE SYSTEM

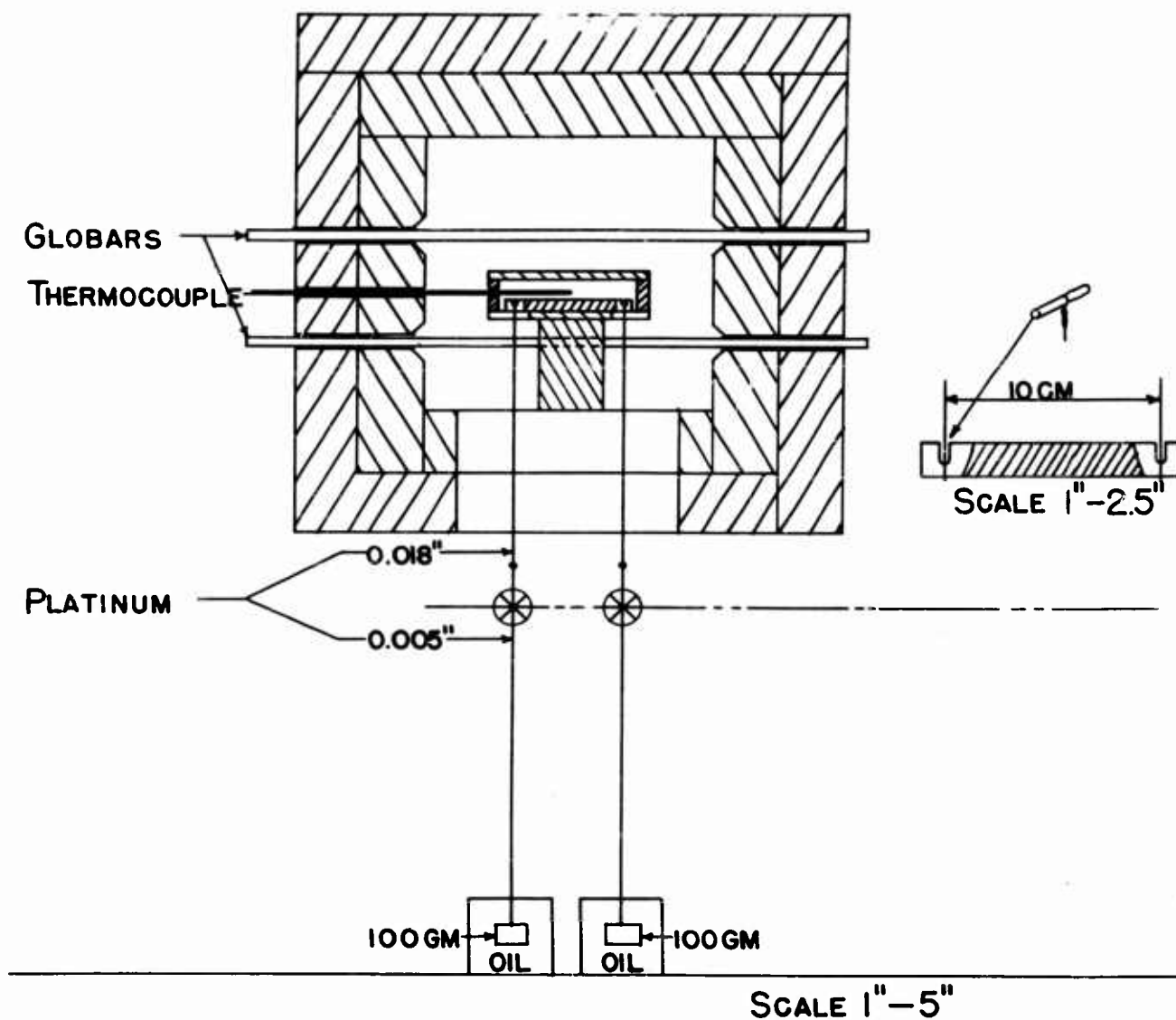


FIG. 9

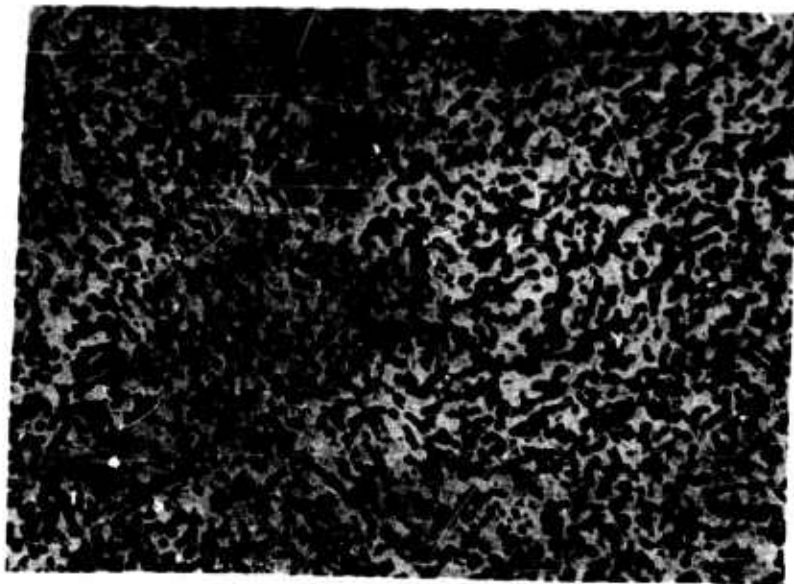


Fig. 10 Sound structure in A-355.6-G. Specimen number 195 at 200X. Black, alumina. White, alloy.



Fig. 11 Globuliferous structure in A-355.6-G Specimen number 207X containing ball-milled alloy at 200X. Black, alumina. White, alloy.

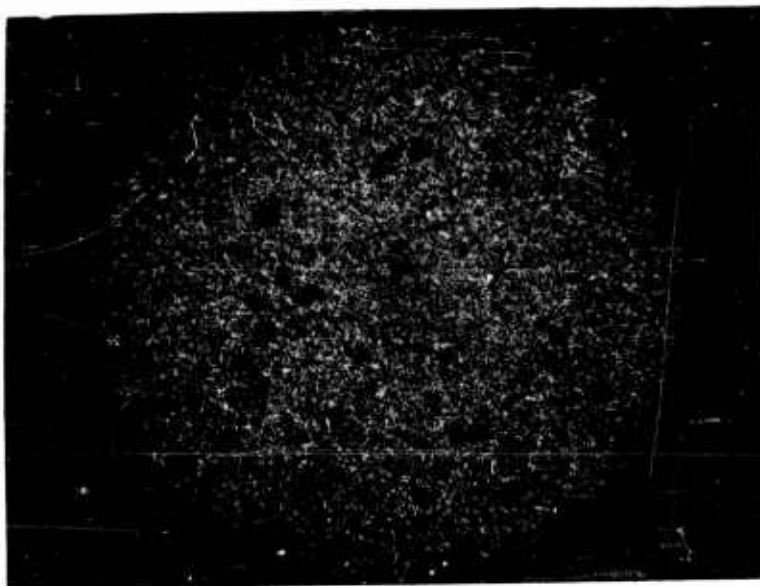


Fig. 12 Condition of segregation in A-355.6-G rod specimen number 9 at 25X. Black, alumina. White, alloy.

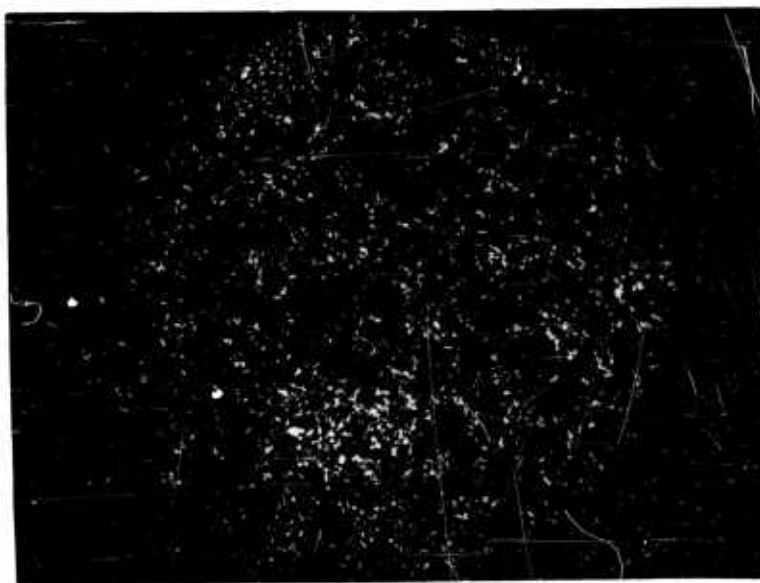


Fig. 13 Microstructure of A-355.6-G solid blade number 4 at 25X. Poorest structure observed in any A-355.6-G specimen. Black, alumina. White, alloy.

Armed Services Technical Information Agency

Because of our limited supply, you are requested to return this copy WHEN IT HAS SERVED YOUR PURPOSE so that it may be made available to other requesters. Your cooperation will be appreciated.

AD

49092

NOTICE: WHEN GOVERNMENT OR OTHER DRAWINGS, SPECIFICATIONS OR OTHER DATA ARE USED FOR ANY PURPOSE OTHER THAN IN CONNECTION WITH A DEFINITELY RELATED GOVERNMENT PROCUREMENT OPERATION, THE U. S. GOVERNMENT THEREBY INCURS NO RESPONSIBILITY, NOR ANY OBLIGATION WHATSOEVER; AND THE FACT THAT THE GOVERNMENT MAY HAVE FORMULATED, FURNISHED, OR IN ANY WAY SUPPLIED THE SAID DRAWINGS, SPECIFICATIONS, OR OTHER DATA IS NOT TO BE REGARDED BY IMPLICATION OR OTHERWISE AS IN ANY MANNER LICENSING THE HOLDER OR ANY OTHER PERSON OR CORPORATION, OR CONVEYING ANY RIGHTS OR PERMISSION TO MANUFACTURE, USE OR SELL ANY PATENTED INVENTION THAT MAY IN ANY WAY BE RELATED THERETO.

Reproduced by
DOCUMENT SERVICE CENTER
KNOTT BUILDING, DAYTON, 2, OHIO

UNCLASSIFIED